Bulletin — 2024 — pp. 52—59

José Alvaro Previato Sardelli, Sérgio Eustáquio Soares and Gláucio Galdino Martins

Microstructural Design Optimisation of Magnesia–Chromite Bricks for RH Degassers: Determining an Optimal Balance Between Thermal Shock and Corrosion Resistance

Magnesia-chromite bricks are widely used in RH degassers due to their outstanding corrosion and abrasion resistance in critical environments. Among the different types of magnesia-chromite bricks, rebonded bricks, characterised by a high fused magnesia-chromite (FMC) content, are particularly preferred in snorkel and throat areas of RH degassers. However, rebonded bricks exhibit lower thermal shock resistance compared to direct-bonded bricks (i.e., based on sintered magnesia and chrome ore). To address this limitation, semi-rebonded bricks have emerged as a potential solution to fulfil these constraints. While the literature has explored the characteristics of these three distinct classes of magnesia-chromite bricks, only a limited number of studies have evaluated the microstructural effects on physical, thermomechanical, and corrosion resistance properties. Therefore, this study aimed to determine the optimal amount of FMC grains to achieve a suitable balance between the required properties. Experimental tests were conducted to assess the impact of increasing amounts of fused grain on the most influential properties of magnesia-chromite bricks. The findings indicated that an optimal quantity of fused grains could be identified, where the physical and thermomechanical properties were improved without compromising corrosion and abrasion resistance, and that these properties could be further enhanced by optimising the grain size distribution (GSD). This study highlights the importance of microstructural differences in formulation design and the selection of appropriate raw materials and GSD to achieve comparable properties to rebonded bricks without influencing essential application requirements.

Introduction

Magnesia-chromite refractories are widely used in various industries due to their exceptional thermal stability, minimal thermal expansion, and resistance to thermal shock. They are particularly favoured in applications such as RH degassers, rotary cement kilns, and nonferrous copper converters [1]. Compared to magnesia-based counterparts, they offer superior thermal shock resistance and corrosion resistance to acidic and basic slags, especially fayalitic slags [1–3]. To improve slag penetration resistance, it is crucial to densify the bricks, reduce apparent porosity, while maintaining thermal shock resistance. This can be achieved through microstructure design, focusing on fostering direct bonding between the refractory grains, including secondary spinel phases and fused magnesia-chromite (FMC), along with a carefully tailored grain size distribution (GSD).

The principal constituents of magnesia-chromite bricks, customised to specific applications, include sintered magnesia, fused magnesia, chrome ore, and FMC. These raw material compositions facilitate categorising magnesia-chromite bricks into three discrete classes: Direct-bonded, semi-rebonded, and rebonded. Each classification presents distinct advantages and constraints, requiring detailed alignment with the specific requisites of the intended application. Notably, direct-bonded bricks exhibit superior thermal shock resistance, but comparatively inferior corrosion resistance compared to rebonded bricks, with the semi-rebonded class filling an intermediate position within this range.

In direct-bonded bricks, the bonding mechanisms between sintered magnesia and chrome ore grains are determined by temperature-driven reactions during the firing process. At 1500 °C, a liquid phase forms around the chrome ore grains, subsequently infiltrating the adjacent magnesia matrix, enabling diffusion of Fe_2O_3, Cr_2O_3, and Al_2O_3 from the chrome ore into the magnesia at 1670 °C. Finally, at 1750 °C, complete dissolution of the chrome ore occurs, precipitating spinel-like exsolution phases within the MgO structure [4]. This behaviour is beneficial for thermal shock resistance owing to the microcracking induced by interdiffusion of chrome ore components into the magnesia matrix.

In the context of RH degassers, magnesia-chromite bricks primarily comprise FMC and are typically classified as rebonded bricks. The main bonding process occurs during the FMC electrofusion process, followed by firing the bricks at temperatures exceeding 1700 °C to form rebonded refractories. The FMC consists mainly of periclase and a solid solution spinel [$(Fe,Mg)(Fe,Al,Cr)_2O_4$], resulting from the fusion of various spinel structures (AB_2O_4-type phases), where A represents a divalent cation and B a trivalent one [5–7]. This complex structure, characterised by interstices and vacancies, enables the formation of solid solutions with broad solubility ranges and ionic radii ranging from 0.44–1.00 Å [5,8]. Consequently, these bricks exhibit excellent resistance to corrosion and slag infiltration. Additionally, preferentially oriented microcracks within the FMC grains enhance the material's flexibility and resistance to thermal shock damage. The FMC features a periclase matrix with

embedded spinel precipitates, typically around 15 µm in size, exhibiting a consistent pattern with {110} planes as revealed by electron backscatter diffraction, aligning with the Zener-Stroh crack mechanism [9]. Figure 1 provides a visual representation of the FMC parameters described.

The semi-rebonded classification of magnesia-chromite bricks involves combining FMC with the microcracking phenomena promoted by the direct-bonded behaviour that occurs between sintered magnesia and chrome ore grains during the firing process. This unique combination has emerged as a promising approach to impart the necessary properties crucial for certain applications. The primary objective of the investigations presented in this paper were to determine the optimal amount of FMC grains necessary to achieve a balanced equilibrium between thermal shock resistance and corrosion resistance, while maintaining the physical and thermomechanical integrity of the material.

Additionally, a secondary aim of the study was to evaluate a new GSD to enhance the microstructure achieved with the optimal amount of FMC.

Materials and Methods

Laboratory magnesia-chromite bricks were formulated utilising Alfred's model incorporating a customised particle size distribution coefficient tailored to the FMC content in the semi-rebonded formulation under investigation. Additionally, a novel GSD was developed and assessed to enhance the key properties of these materials during application. A spectrum of compositions ranging from low to high FMC content was systematically explored (Table I). To ensure comparison across all FMC compositions and mitigate any potential interference during firing, uniform binder systems and sintering additives were incorporated across all compositions.

Figure 1.

Morphology and elemental mapping of the FMC microstructure assessed by scanning electron microscopy coupled with energy dispersive spectroscopy [9].

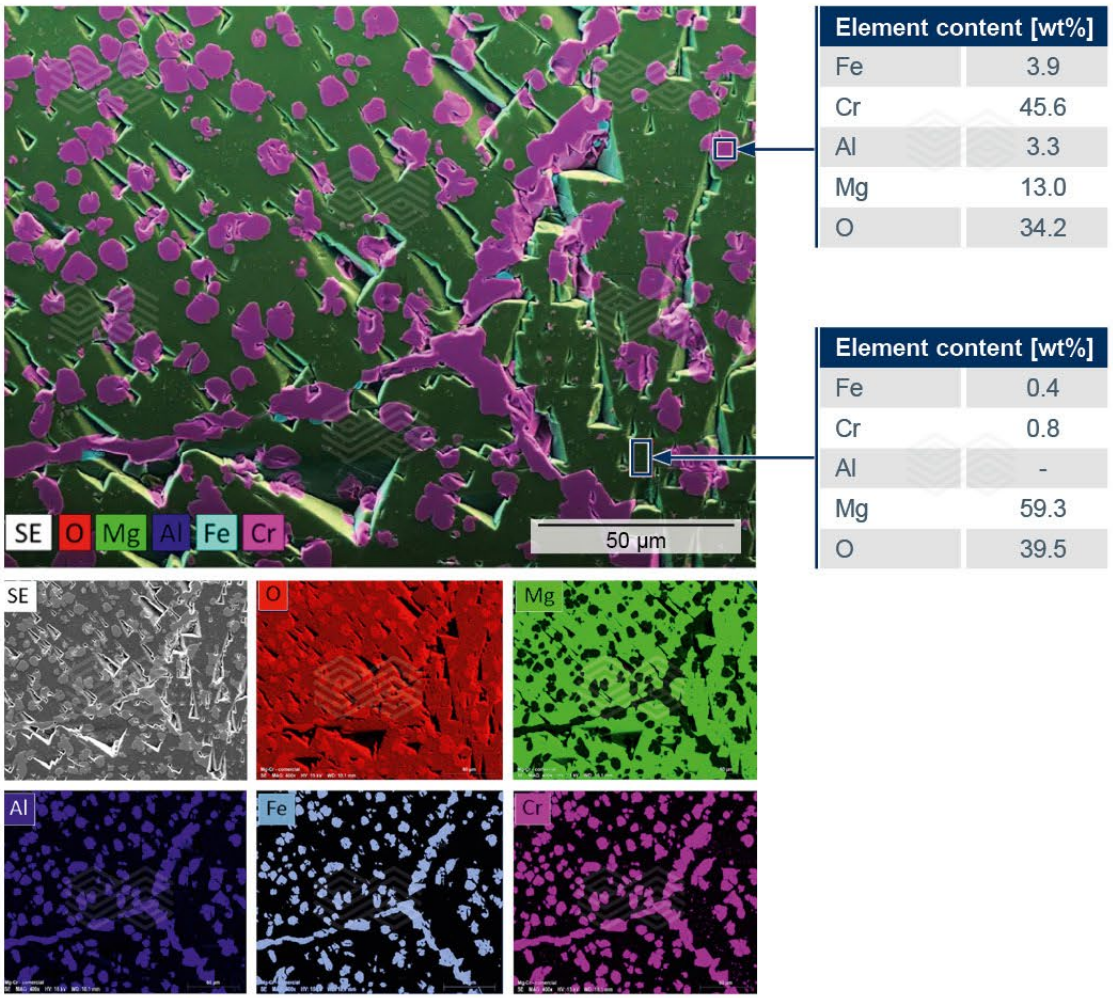

Element content [wt%]	
Fe	3.9
Cr	45.6
Al	3.3
Mg	13.0
O	34.2

Element content [wt%]	
Fe	0.4
Cr	0.8
Al	-
Mg	59.3
O	39.5

Table I.

Compositions evaluated during the semi-rebonded magnesia-chromite brick development.

Grain size distribution	Raw materials	A	B	C	D	E	F
Standard GSD	FMC content	+	++	+++	++++	+++++	++++++
New GSD	FMC content	+	++	+++	++++	+++++	++++++

All formulations were homogenised in roller mixers and hydraulic presses were used to shape 160 x 85 x 63 mm^3 bricks that were subsequently fired at temperatures above 1700 °C in an industrial tunnel kiln. Bulk density and apparent porosity were determined using a liquid immersion method in water, according to the ABNT NBR 6220 standard. Cold modulus of rupture was evaluated using a KRATOS KE (3 tonnes) and cold crushing strength was carried out with a KRATOS ECC (Brazil) using a 100 kN load cell (JIS, R-2206, Brazil) on cylindrical 50 x 50 mm^3 specimens. Hot modulus of rupture was carried out on bars (152 x 25 x 25 mm^3) placed in an electric furnace with a continuous sample feeding system coupled to a mechanical press (KRATOS K500/2000, Brazil). The permeability test was conducted according to ASTM C577 and abrasion resistance was measured following ASTM C704. Microstructure analysis by optical microscopy was carried out using a Carl Zeiss microscope (AXIO-Imager model). The thermal shock resistance test was conducted on 152 x 25 x 25 mm^3 bars using a water-cooled copper plate. The decrease of elastic modulus was followed for 5 thermal shock cycles (ΔT = 700 °C) (ABNT NBR 13202) utilising ultrasound equipment (Emodumeter, James Instruments, USA). Based on the ultrasound velocity and density of each sample, the elastic modulus was calculated as well as the residual elastic modulus at the end of 5 cycles. Additionally, the residual modulus of rupture was measured after the 5th cycle. The corrosion tests were performed at 1700 °C in an induction furnace, using steel and fayalitic slag added every 30 minutes for 5 hours, and 8 samples were evaluated simultaneously.

Laboratory Trial Results

To assess the impact of different levels of FMC and the two GSDs on bulk density and apparent porosity, 3 samples of each magnesia-chromite brick composition were tested. Based on the results obtained, it was apparent that increasing the FMC content led to an overall rise in bulk density, coupled with a decline in apparent porosity for both GSDs examined (Figure 2). Furthermore, alongside the benefits of increasing the high-grade raw material content on these properties, the new GSD emerged as a pivotal factor for increasing bulk density and decreasing porosity, apart from at the lowest level of FMC addition.

To visually examine the different brick compositions, optical microscopy was performed and micrographs of compositions featuring the standard GSD are provided in Figure 3. The images clearly demonstrate how each composition's microstructure changes with the addition of higher FMC levels; most notably the porosity decreases, leading to improved densification.

Figure 2.

Bulk density (BD) and apparent porosity (AP) of the different magnesia-chromite brick compositions with increasing amounts of FMC and two GSDs. The lines between the AP values are for visual guidance.

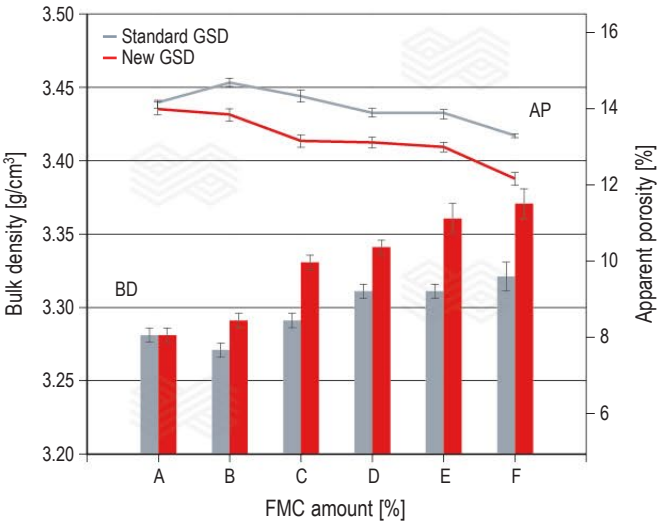

Figure 3.

Comparative microstructural evaluation of fired magnesia-chromite bricks with different FMC content and the standard GSD. The images (a–f) correspond to the increased addition of FMC as detailed in Table I. FMC (1), sintered magnesia (2), and chromite (3) are indicated.

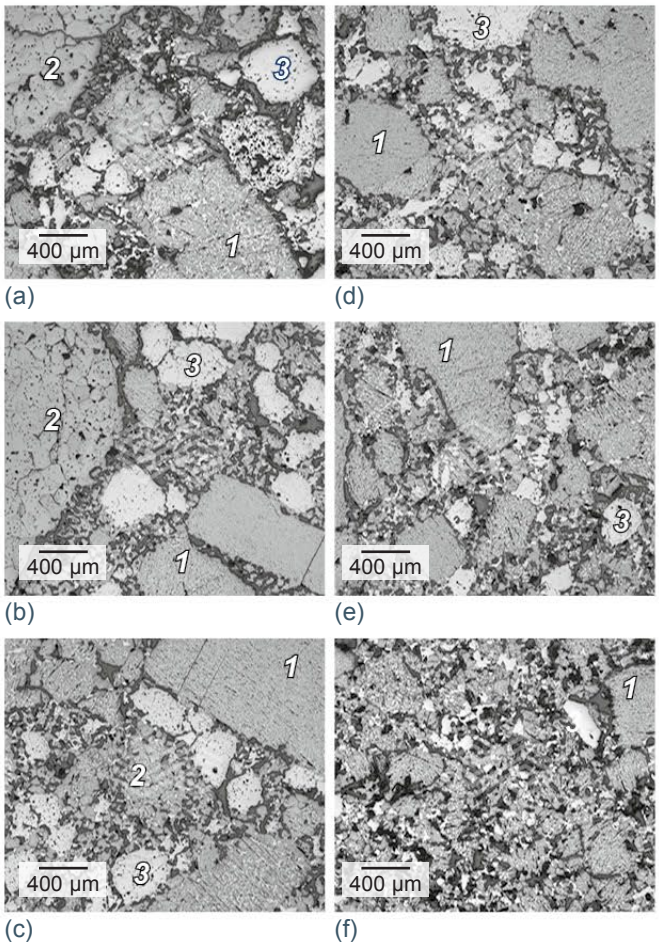

In order to explore the influence of FMC content and GSD on cold mechanical properties, the cold crushing strength and cold modulus of rupture were measured for 3 samples of each magnesia-chromite brick composition. The results presented in Figure 4 show that both properties increased with FMC content for both GSDs. However, regarding the cold crushing strength, discernible differences in values between the two GSD only emerged from composition D onwards, with the magnitude of difference increasing with FMC content. In summary, it appeared that the novel GSD effectively optimised microstructural packing, resulting in highly favourable outcomes for practical applications when combined with higher amounts of FMC. In contrast, a similar trend was not observed for the cold modulus of rupture. Although at the lowest FMC content no distinction was observed between the GSDs, for all other compositions the standard distribution exhibited a higher cold modulus of rupture compared to the new GSD.

To assess the influence of FMC addition and GSD on thermomechanical properties, the hot modulus of rupture test was conducted on 3 samples of each brick composition at test temperatures of 1250 °C, 1400 °C, and 1485 °C (Figure 5). At 1250 °C, the hot modulus of rupture showed an upward trend with the increasing addition of FMC, irrespective of the GSD, indicating incorporation of FMC had a beneficial effect on this thermomechanical property, while the GSD did not significantly influence the obtained values. With an elevation of the test temperature to 1400 °C, the hot modulus of rupture was lower than at 1250 °C, but also rose with increasing amounts of FMC, in a similar manner for both GSDs, until a certain content was reached (i.e., composition D), whereupon this upward trend stabilised. It is established that at 1400 °C, liquid phase formation originating from in situ generated silicate minerals (e.g., monticellite and merwinite) is more prevalent in the material's microstructure, which would account for the observations. At a testing temperature of 1485 °C all the samples showed the lowest hot modulus of rupture, with similar values irrespective of FMC content and GSD.

Figure 4.

Cold crushing strength (CCS) and cold modulus of rupture (CMOR) of the different magnesia-chromite brick compositions with increasing amounts of FMC and two GSDs. The lines connecting the CMOR values are for visual guidance.

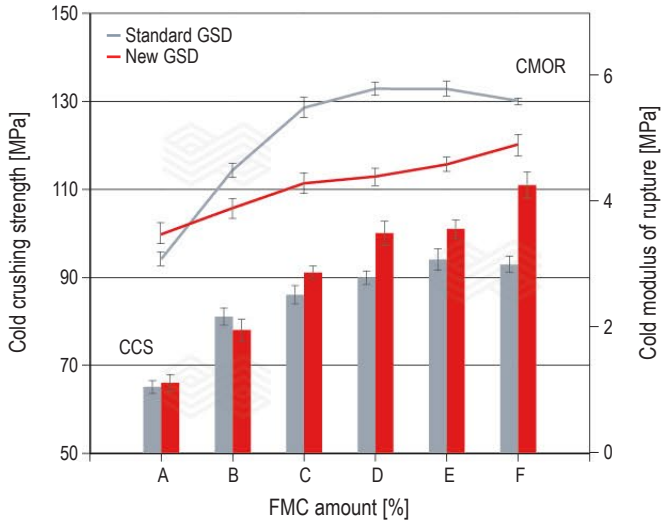

The microcracking effect induced by direct-bonding reactions within the magnesia-chromite brick matrix is an approach to enhance thermal shock resistance, when appropriately balanced against corrosion by slag and molten metal. To examine the influence of FMC content and GSD on thermal shock behaviour, 3 samples of each magnesia-chromite brick composition were heated to 725 °C, held for 30 minutes, and rapidly cooled to room temperature. After each thermal cycle, the elastic modulus was determined and after 5 cycles the residual elastic modulus was calculated. In addition, the cold modulus of rupture was measured at the end of the 5 cycles and the residual cold modulus of rupture determined. The residual elastic modulus results (Figure 6)

Figure 5.

Hot modulus of rupture (HMOR) of the different magnesia-chromite brick compositions with increasing amounts of FMC and two GSDs, tested at 1250 °C, 1400 °C, and 1485 °C. The bars correspond to the standard GSD at the three test temperatures and the squares, triangles, and circles to the new GSD at 1250 °C, 1400 °C, and 1485 °C, respectively. The lines connecting the HMOR values of the new GSD are for visual guidance.

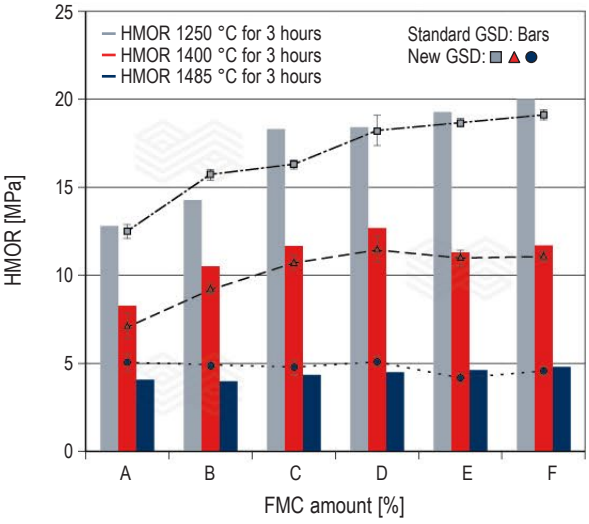

Figure 6.

Residual elastic modulus (EM) and residual cold modulus of rupture (CMOR) of the different magnesia-chromite brick compositions with increasing amounts of FMC and two GSDs after 5 thermal shock cycles (i.e., 725 ºC to room temperature). The lines connecting the residual CMOR values are for visual guidance.

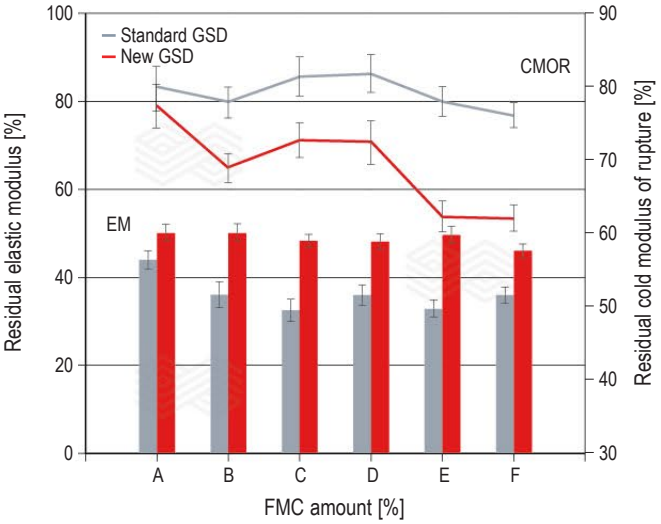

indicate that increasing the FMC content was not detrimental to the thermal shock behaviour and that the new GSD positively impacted this property. However, the residual cold modulus of rupture showed a decreasing trend with increased FMC addition, which was more pronounced with the standard GSD.

Having determined that the thermal shock resistance was not detrimentally affected in materials featuring high FMC levels corresponding to direct-bonded compositions, it was essential to evaluate the impact of FMC addition on other pertinent properties, notably corrosion resistance. However, a critical aspect to enhancing this essential property entails understanding the material's permeability and abrasion characteristics, which in conjunction with chemical corrosion are key factors contributing to the compromised performance of magnesia-chromite bricks. Figure 7 shows the permeability and abrasion values obtained for 3 samples of each magnesia-chromite brick composition, indicating the permeability slightly decreased with FMC addition, irrespective of the GSD, and that abrasion was notably lower for both GSDs with increasing FMC content.

The final analyses performed on all the different magnesia-chromite brick compositions were corrosion tests conducted at 1700 °C for 5 hours with steel and fayalitic slag. It is important to mention that it was not possible to evaluate all 12 brick compositions simultaneously due to the experimental setup; however, multiple tests were conducted and wear in both the steel and slag zones was assessed. The results presented in Figure 8 show that in both the slag and steel zones, typically an increased FMC content positively influenced the corrosion resistance, with a significant benefit observed for the new GSD in the slag zone.

Plant Implementation Results

Following the culmination of research and development activities aimed at creating a new magnesia-chromite grade endowed with optimal properties and an engineered microstructure, composition D was selected for plant trials. One-tonne mixes of both the standard and new GSD were processed in an industrial mixer, pressed into RH degasser throat shapes, and fired according to standard plant procedures. Subsequently, the properties of five bricks for each GSD were determined and the results compared to those of the laboratory-produced bricks (Table II). In the

Table II.

Comparison of the results obtained for laboratory and plant trial bricks produced using composition D with either the standard or new grain size distribution (GSD).

Composition D	Laboratory trial bricks		Plant trial bricks	
Properties	Standard GSD	New GSD	Standard GSD	New GSD
BD [g/cm^3]	3.31	3.34	3.34	3.36
AP [%]	13.90	13.13	13.37	12.37
CCS [MPa]	90	100	133	125
CMOR [MPa]	5.8	4.4	8.3	8.7
HMOR 1250 °C [MPa]	18.4	18.2	18.0	17.2
HMOR 1400 °C [MPa]	12.7	11.5	9.9	13.7
HMOR 1485 °C [MPa]	4.5	5.1	4.4	5.3
Abrasion [%]	14.5	14.9	8.0	7.7
Permeability [cD]	43.5	48.1	36.3	37.8
Thermal shock resistance (ΔT = 700 °C)				
Residual EM [%]	36.0	48.1	47.0	48.0
Residual CMOR [%]	72.3	83.0	72.4	81.8
Corrosion test (induction furnace at 1700 °C for 5 hours)				
Metal line [%]	6.19	4.72	5.50	5.76
Slag line [%]	52.08	32.30	42.79	39.35

Figure 7.

Permeability and abrasion of the different magnesia-chromite brick compositions with increasing amounts of FMC and two GSDs. The lines connecting the abrasion values are for visual guidance.

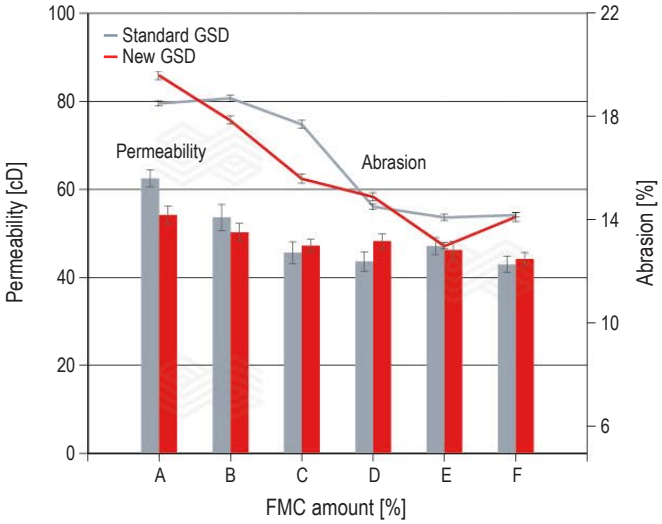

Figure 8.

Corrosion of the different magnesia-chromite brick compositions with increasing amounts of FMC and two GSDs observed in the slag and steel zones after 5 hours at 1700 °C in an induction furnace. The bars correspond to corrosion of the standard GSD in the slag and steel zones and the triangles and squares to corrosion of the new GSD in the slag and steel zones, respectively. The lines connecting the corrosion percent of the new GSD are for visual guidance.

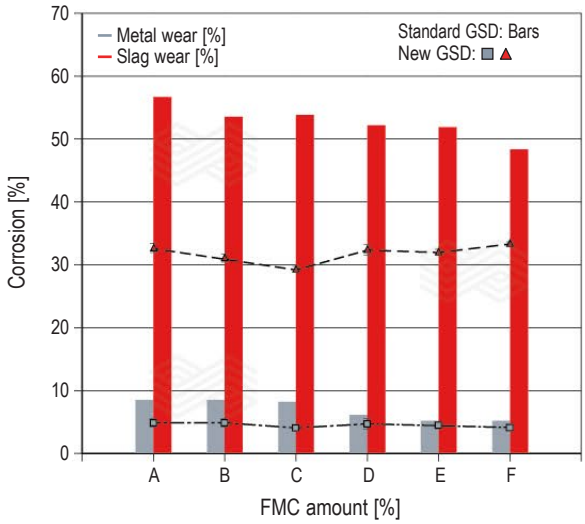

majority of cases, properties of the plant trial bricks were either equivalent or better than the laboratory-produced bricks, with the only notable exceptions related to the hot modulus of rupture. Furthermore, properties of the plant trial bricks with the new GSD were typically better than the standard GSD. Microscopy was also performed and showed that bricks produced in the plant with the new GSD had a dense microstructure (Figure 9). Consequently, composition D featuring the new GSD (i.e., RADEX TB016) was selected for field trials in the throat area of RH degassers at six Brazilian customers.

Customer Trial Results

Currently, only one of the six Brazilian customers has completed field trials with the developed material. In this case, the initial test was carried out in the outlet throat (down leg) of the RH degasser. Throughout this campaign, which ran for 78 heats and ended based on the customer's program, the field trial was documented in detail, as shown in Figures 10–12. Given that the outlet throat typically experiences lower stresses than the inlet throat (up leg), conducting a field trial in the less demanding region was an

Figure 9.

Microstructural evaluation of RADEX TB016, a fired magnesia-chromite brick produced during the plant trial (i.e., composition D) with the new GSD. The images (a–c) show a dense microstructure and FMC (1), sintered magnesia (2), and chromite (3) are indicated.

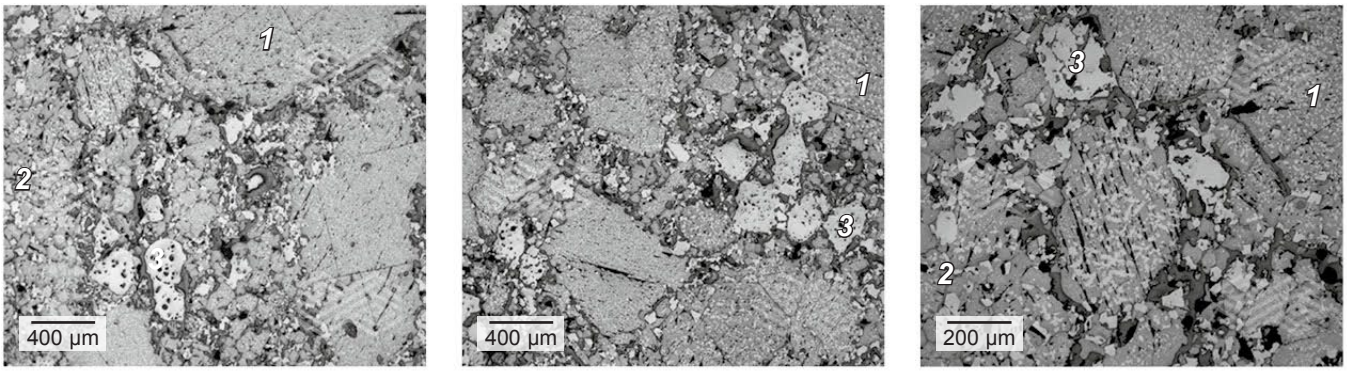

(a) (b) (c)

Figure 10.

RH degasser showing (a) installation of RADEX TB016 in the outlet throat and a standard magnesia-chromite grade in the inlet throat and (b) completed installation.

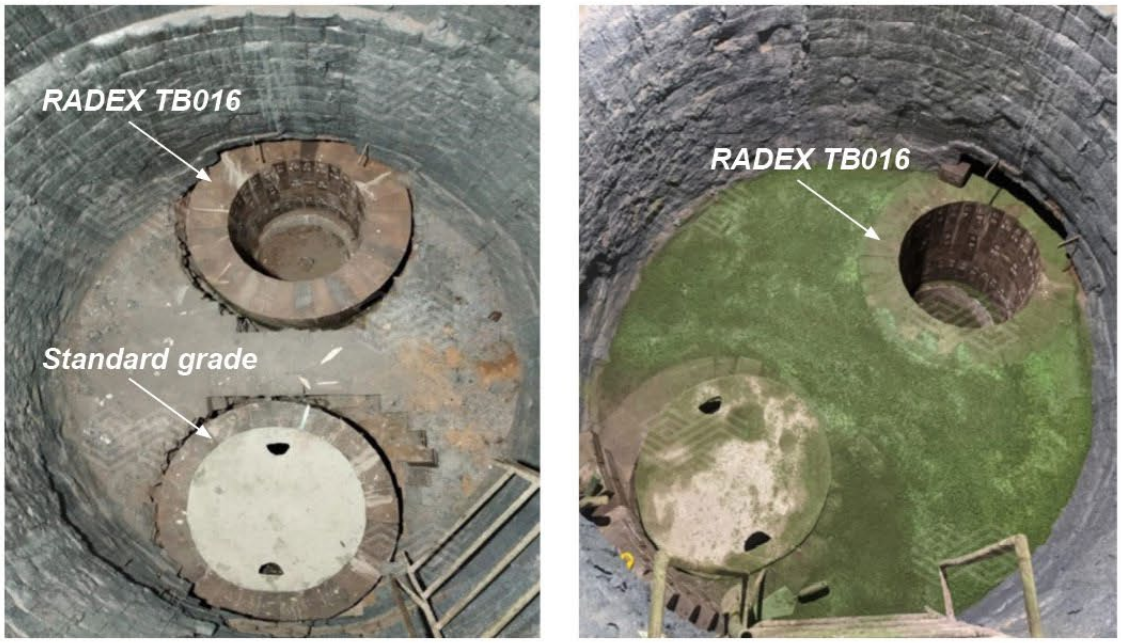

(a) (b)

appropriate first step to evaluate the new grade. During the trial, the RADEX TB016 exhibited minimal wear with residual thicknesses ranging from 225 mm (initial brick dimension) to 190 mm. Furthermore, the RADEX TB016 bricks showed significantly less wear compared to the standard magnesia-chromite bricks from another supplier used to line this area. Figure 11 shows the visual appearance of the outlet throat lined with RADEX TB016 during the campaign. The calculated wear rate of RADEX TB016 was 0.385 mm/hour, indicating a potential throat lifetime of up to 415 heats with this new grade, while maintaining a minimum safety thickness of 60 mm. Following the initial field trial, RADEX TB016 was successfully implemented in the inlet throat for a campaign of 104 heats, which ended according to the customer-defined process.

Figure 11.

Images of the RH degasser outlet throat region lined with the RADEX TB016 at (a) 22 heats, (b) 34 heats, (c) 52 heats, and (d) 78 heats during the campaign.

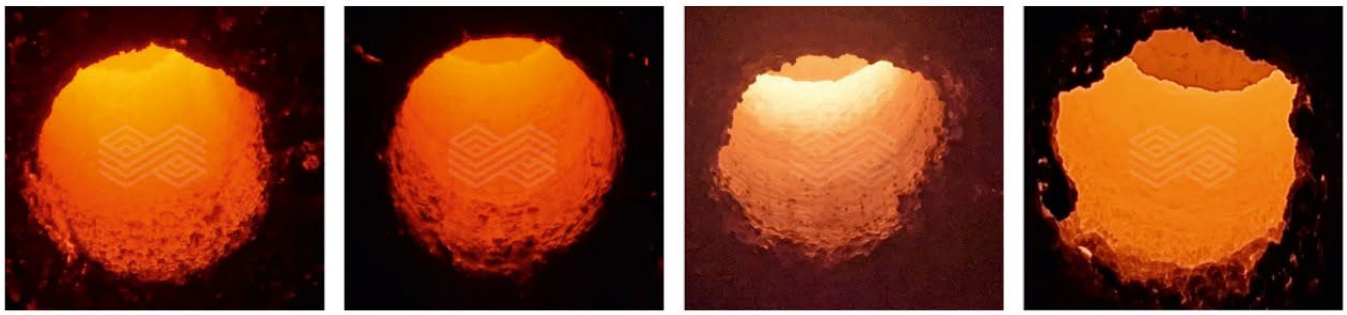

(a) (b) (c) (d)

Figure 12.

(a) lining disassembly of the outlet throat region lined with RADEX TB016 enabling measurement of (b) the residual brick thicknesses that ranged from 190–195 mm.

(a) (b)

Conclusion

Magnesia-chromite bricks, incorporating increasing amounts of FMC as a substitute for sintered magnesia and chrome ore, were produced on a laboratory scale and comprehensively evaluated. In addition, the impact of two distinct GSDs on the various magnesia-chromite brick compositions was also assessed. The results indicated that regarding essential properties for magnesia-chromite brick applications, the addition of FMC enhanced these properties, underscoring the importance of rebonded magnesia-chromite bricks for various demanding applications. Furthermore, the other parameter investigated in this study demonstrated the potential for property enhancement not only through high-quality raw materials but also by optimising the GSD. Following extensive comparative analysis of numerous compositions during the developmental phase, composition D was chosen for plant trials with both the standard and new GSD. Although most of the properties measured for the bricks produced with both GSDs in the plant were better than the laboratory-scale equivalent, particularly notable improvements were observed with the new GSD. Consequently, composition D featuring the new GSD (i.e., RADEX TB016) was selected for field trials at six Brazilian steel plants in the RH degasser. Recently, trials at one customer were completed and showed excellent performance of RADEX TB016 in the outlet and inlet throats, with the potential to increase the RH degasser's lifetime. In conclusion, the newly developed magnesia-chromite grade, RADEX TB016, further extends RHI Magnesita's portfolio of high-performance refractory grades for RH degassers.

References

[1] Azhari, A., Golestani-Fard, F. and Sarpoolaki, H. Effect of Nano Iron Oxide as an Additive on Phase and Microstructural Evolution of Mag-Chrome Refractory Matrix. *J. Eur. Ceram. Soc*. 2009, 29, 2679–2684.
[2] Goto, K. and Lee, W. E. The "Direct Bond" in Magnesia Chromite and Magnesia Spinel Refractories. *J. Am. Ceram. Soc*. 1995, 78, 1753–1760.
[3] Alper, A.M. (Ed.). *High Temperature Oxides*; Academic Press: New York, 1970.
[4] Guo, Z. and Ma, Y. Bonding Mechanisms of Basic Refractories for RH Snorkels. Presented at the 16th United International Technical Conference on Refractories (UNITECR), Yokohama, Japan, Oct. 13–16, 2019.
[5] Landy, R.A. *Magnesia Refractories. In: Refractories Handbook*; CRC Press, 2004, 109–149.
[6] Xu, T., Xu, Y., Li, Y., Sang, S., Wang, Q., Zhu, T., Nath, M. and Zhang, B. Corrosion Mechanisms of Magnesia-Chrome Refractories in Copper Slag and Concurrent Formation of Hexavalent Chromium. *J. Alloy. Compd*. 2019, 786, 306–313.
[7] Zhu, D., Yang, C., Pan, J., Zhang, Q., Shi, B. and Zhang, F., Insight into the Consolidation Mechanism of Oxidized Pellets Made from the Mixture of Magnetite and Chromite Concentrates. *Metall. Mater. Trans. B*. 2016, 47, 1010–1023.
[8] Brosnan, D.A. *Corrosion of Refractories. In: Refractories Handbook*; CRC Press, 2004, 39–78.
[9] Borges, O. H., Coury, F. G., Muche, D. N. F. and Pandolfelli, V. C., Eco-Friendly Design of Complex Refractory Aggregates as Alternatives to the Magnesia-Chromite Ones. *J. Eur. Ceram. Soc*. 2023, 43, 6536–6549.

Authors

José Alvaro Previato Sardelli, RHI Magnesita, Contagem, Brazil.
Sérgio Eustáquio Soares, RHI Magnesita, Contagem, Brazil.
Gláucio Galdino Martins, RHI Magnesita, Contagem, Brazil.
Corresponding author: José Alvaro Previato Sardelli. Jose.Sardelli@rhimagnesita.com

Bulletin

The Journal of Refractory Innovations

2024

Published by RHI Magnesita GmbH, Vienna, Austria
Chief Editor Thomas Prietl
Executive Editors Celio Carvalho Cavalcante, Thomas Drnek, Christoph Eglsäer, Celso Freitas, Alexander Leitner, Ravikumar Periyasamy, Stefan Postrach, Peter Steinkellner, Karl-Michael Zettl
Raw Materials Expert Matheus Naves Moraes
Technical Proofreader Clare McFarlane
Lingual Proofreader Clare McFarlane
Project Manager Michaela Hall
Design and Typesetting Universal Druckerei GmbH, Leoben, Austria

Contact Michaela Hall
RHI Magnesita GmbH, Technology Center
Magnesitstrasse 2
8700 Leoben, Austria

E-mail bulletin@rhimagnesita.com
Phone +43 50213 5300
Website rhimagnesita.com
LinkedIn https://www.linkedin.com/company/rhi-magnesita

Cover picture: The image depicts the lower section of a RH degasser, a secondary metallurgical unit used in steel plants. In the RH degassing process, snorkels are submerged into liquid steel contained in the casting ladle. Argon gas is purged through the inlet snorkel, creating a suction effect that draws liquid steel into the lower vessel of the RH degasser, where a vacuum is applied. The steel treated in the lower vessel flows back to the ladle through the outlet snorkel, creating a continuous steel circulation between the ladle and the RH degasser. The strong negative pressure (vacuum) within the RH degasser facilitates various metallurgical processes that enhance steel quality, with the key process steps including degassing, decarburisation, deoxidation, and alloying under vacuum. Rail steel, flat steel for the automotive industry, and steel plates for shipbuilding are just a few examples of products that benefit from the RH degasser. Prefabricated snorkels, which RHI MAGNESITA manufactures ready for use and delivers to our globally operating customers, are essential components of the RH degasser.